Structural Insights into Human 5-Lipoxygenase Inhibition: Combined Ligand-Based and Target-Based Approach

Caroline Charlier,[†] Jean-Pierre Hénichart,[‡] François Durant,[†] and Johan Wouters[†,*]

Laboratory of Structural Biological Chemistry, University of Namur, FUNDP, 61, rue de Bruxelles, B-5000 Namur, Belgium, and Institut de Chimie Pharmaceutique Albert Lespagnol, EA 2692, Université de Lille 2, BP 83, F-59006 Lille, France

Received September 2, 2005

The human 5-LOX enzyme and its interaction with competitive inhibitors were investigated by means of a combined ligand-based and target-based approach. First, a pharmacophore model was generated for 16 non redox 5-LOX inhibitors with Catalyst (HipHop module). It includes two hydrophobic groups, an aromatic ring, and two hydrogen bond acceptors. The 3D structure of human 5-LOX was then modeled based on the crystal structure of rabbit 15-LOX, and the binding modes of representative ligands were studied by molecular docking. Confrontation of the docking results with the pharmacophore model allowed the weighting of the pharmacophoric features and the integration of structural information. This led to the proposal of an interaction model inside the 5-LOX active site, consisting of four major and two secondary interaction points: on one hand, two hydrophobic groups, an aromatic ring, and a hydrogen bond acceptor, and, on the other hand, an acidic moiety and an additional hydrogen bond acceptor.

Introduction

Lipoxygenases (LOX) constitute a heterogeneous family of lipid-peroxidizing enzymes, widely distributed in plants and mammals but also in fungi and invertebrates.[1,2] More recently, it has also been discovered in bacteria.[3,4] These dioxygenases catalyze the regio- and stereospecific insertion of molecular oxygen to polyunsaturated fatty acids containing one or more (*Z*,*Z*)-1,4-pentadiene moieties, leading to hydroperoxy derivatives.[5] They require one non-heme iron atom per molecule, which oscillates between Fe^{2+} (inactive) and Fe^{3+} (active) states. The role for iron in the generally accepted LOX reaction mechanism is to act as electron acceptor and donor, during hydrogen abstraction and peroxide formation. In the animal kingdom, four major isoforms have currently been identified. They include the 5-, 8-, 12-, and 15-LOX. Historically, these are classified according to their positional specificity of oxygenation of arachidonic acid (AA), their main substrate.

LOX metabolites are potent physiological effectors in a variety of cellular responses, associated with normal host defense and inflammation. In particular, leukotrienes (LTs) are produced through the 5-LOX pathway. Upon cell activation, 5-LOX converts AA to 5-hydroperoxy-6,8,11,14-eicosatetraenoic acid (5-HPETE) and afterward into the epoxide LTA_4.[6] The subsequent conversion of LTA_4 by LTA_4 hydrolase gives LTB_4, whereas metabolism by LTC_4 synthase yields the cysteinyl-LTs C_4, D_4, and E_4. LTs are critical mediators of immediate hypersensitivity reactions and inflammation.[7,8] They are involved in numerous inflammatory diseases and allergic disorders, such as allergy, asthma, arthritis, and psoriasis.[9,10] Moreover, recent studies suggest a role of 5-LOX products also in carcinogenesis and cell survival,[11,12] and in atherosclerosis.[13,14] Regarding these diverse biological properties, the inhibition of this metabolic pathway is particularly interesting for the treatment of asthma and inflammatory diseases but may also have potential in the treatment of pancreatic and prostate cancer, and atherosclerosis.

To date, various chemical families of 5-LOX inhibitors have been described in the literature, classified depending on their mechanism of action. Three different types of inhibitors can be considered: (i) antioxidant agents that interfere with the redox catalytic cycle of the enzyme, (ii) iron-chelating agents, and (iii) non redox competitive inhibitors, which compete with the substrate to bind the active site.[15,16] Currently, an emerging strategy of therapeutic value consists of creating molecules with a dual activity, in particular, 5-LOX/COX inhibitors (antiinflammatory)[17] and agents with 5-LOX enzyme inhibition and histamine H1 receptor antagonist properties (antiasthmatic).[18,19] These are thought to be more potent than classical inhibitors and potentially responsible for fewer side effects.

In a view to help in the design of such compounds, structural insight into 5-LOX active site and its interaction with ligands is of particular interest. As the crystal structure of the protein has yet to be elucidated, modeling studies are helpful to obtain a consistent representation of the enzyme−inhibitor recognition step at the molecular level and furthermore, provide new insights that can be used to design novel therapeutic agents.

In this paper, the human 5-LOX enzyme and its interaction with competitive non redox inhibitors were investigated by means of a combined ligand-based and target-based approach, consisting of (1) pharmacophore modeling of non redox 5-LOX inhibitors, (2) homology modeling of human 5-LOX 3D structure, and (3) docking of selected representative inhibitors.

Results and Discussion

Pharmacophore Modeling. Pharmacophore modeling requires molecules showing a large variety in chemical structure and which interact through the same binding mechanism with the target of interest. Therefore, among the three types of 5-LOX inhibitors known (redox, iron chelators, and non redox), we chose to focus solely on the latter non redox compounds. Because of their inability to interfere in redox processes, these active-site directed inhibitors have been shown to be more potent and selective than redox and iron chelating agents and thus prone to fewer side effects.[20]

To date, few non redox 5-LOX inhibitors have been described in the literature, which are structurally different. The three main

* To whom correspondence should be addressed. Tel.: + 32 (0)81 72 45 50. Fax: + 32 (0)81 72 45 30. E-mail: johan.wouters@fundp.ac.be.
[†] University of Namur.
[‡] Université de Lille 2.

10.1021/jm050870x CCC: $33.50
Published on Web 11/24/2005

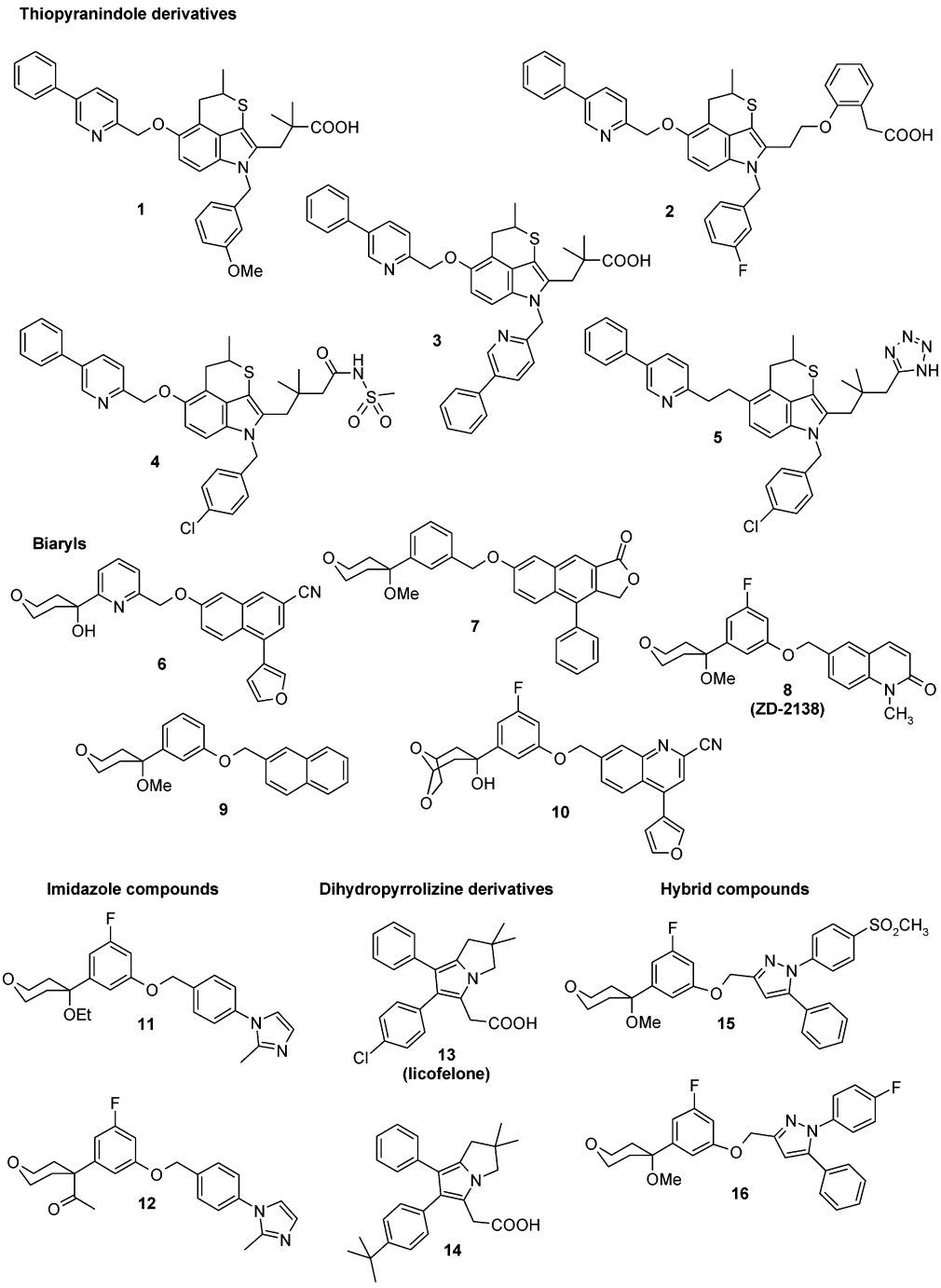

Figure 1. Chemical structures of representative non redox 5-LOX inhibitors (**1**−**12**) and dual 5-LOX/COX inhibitors (**13**−**16**) considered as training set molecules for pharmacophore modeling. Compounds **1**, **6**, **11**, **13**, and **15** were also included in docking studies.

families that we considered for pharmacophore generation (Figure 1) comprise (i) the thiopyranindole derivatives,[21] (ii) the biaryls,[22] and finally (iii) the imidazole compounds.[23] Because of the restricted range of 5-LOX inhibition activities exhibited by all the inhibitors at our disposal, plus the fact that these activities originate from different procedures (Table 1), we decided not to generate quantitative structure−activity relationships. However, the selected molecules represent a pool of potent inhibitors acting on the same target with a similar mechanism (non redox). Therefore, we applied the HipHop process from Catalyst software, which compares diverse and highly active inhibitors to derive 3D hypotheses based on common chemical features, without considering biological activities. To enhance the structural diversity, in addition to the three principal non redox 5-LOX inhibitors families, we also took into account two classes of dual 5-LOX/COX inhibitors (Figure 1) which have been shown to exhibit the same non redox mode of action. It involves (i) dihydropyrrolizine derivatives,[24] among which licofelone (**13**) is the dual 5-LOX/COX inhibitor the most advanced in clinical development for the treatment of osteoarthritis,[25] and (ii) hybrid compounds derived from the associative synthesis of 5-LOX and COX-2 pharmacophoric features, namely the methoxytetrahydropyran of ZD-2138 (**8**) and the classic tricyclic methanesulfone (celecoxib-like) of selective COX-2 inhibitors.[26,27]

The final training set consisting of 16 diverse and highly active inhibitors was submitted for pharmacophore building. The 10 pharmacophore hypotheses generated consisted of five features and had scores ranging from 155 to 163. Three groups emerged based on hierarchical clustering of all 10 hypotheses:

Table 1. Activities of the Selected Compounds, Originating from Three Main Types of Biological Assays, i.e. Enzymatic, Cellular, and Human Whole Blood (expressed in terms of IC_{50})

compd	enzymatic assay IC_{50} (nM)	cellular assay IC_{50} (nM)	HWB[f] IC_{50} (nM)	ref
1	40[a]	28[c]	-	21
2	23[b]	-	-	28
3	30[a]	16[c]	-	21
4	36[a]	11[c]	-	21
5	16[a]	3[c]	-	21
6	15[b]	0.6[c]	30	22
7	14[b]	1.5[c]	50	29
8	330[b]	10[c]	80	29
9	10[b]	1.2[c]	60	29
10	27[b]	2.3[c]	36	30
11	-	-	80	23
12	-	-	130	23
13	-	180[d]	-	24
14	-	180[d]	-	24
15	-	3[e]	300	26,27
16	-	-	480	26

[a] Rat 5-LOX. [b] Human 5-LOX. [c] HPMNL = human polymorphonuclear leukocytes. [d] BPMNL = bovine polymorphonuclear leukocytes. [e] Granulocytes-like cells. [f] HWB = human whole blood.

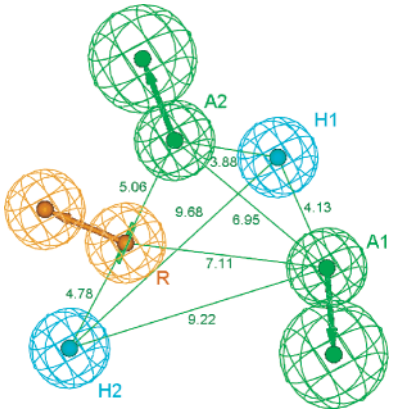

Figure 2. Selected pharmacophore hypothesis for non redox 5-LOX inhibitors consisting of two hydrogen bond acceptors A (green), two hydrophobic groups H (cyan), and an aromatic ring R (orange). Distances between the features are expressed in Å, with a tolerance of ±0.8 Å.

RHHAA, RZHAA, and ZHHAA. The hypotheses differ mainly in the features locations and/or the hydrogen bond vectors direction. Of the 10 pharmacophore models, the sixth was considered as the most relevant since it best corroborates the structure−activity relationships (SAR) available in the literature for the different inhibitors. It consists of two hydrophobic groups (H), two hydrogen bond acceptors (A) and an aromatic ring (R) (Figure 2).

The representation of the chemical features mapped onto representative studied inhibitors is depicted in Figure 3. Hydrophobic functions (H1 and H2) are defined by either aliphatic groups, such as methyl, or aromatic moieties, like phenyl and furan, or halogen atoms. The aromatic ring (R) involves phenyl, indole, pyrazole, or naphthalene moiety, and finally the hydrogen bond acceptors (A1 and A2) consist of either oxygen atom in ether, tetrahydropyran ring, and carboxylic acid group, or sulfur atom in thiopyran ring.

Licofelone **13**, one of the dihydropyrrolizine derivatives, is smaller than the other inhibitors and contains only one hydrogen bond acceptor. This was taken into account in our pharmacophore hypothesis generation methodology (see Computational Methods for details). Since the model derived in this study does not include activity values, it is difficult to speculate if the lack of mapping both A by licofelone accounts for its slightly lower inhibitory potency against 5-LOX (Figure 3).

To determine how well the pharmacophore fits the active site of human 5-LOX, a 3D structure of the enzyme was constructed by homology modeling. Confrontation of both results should allow us to refine the pharmacophore by including structural features derived from the 5-LOX active site.

Homology Modeling. Homology modeling uses experimentally determined protein structures (templates) to predict the conformation of another protein (target) that presents a similar or homologous amino acid sequence. This method generally consists of four major sequential steps: (1) selection of the template(s), i.e., protein(s) with known 3D structure and a similar sequence, (2) target/template sequence alignment, (3) building of the model and subsequent optimization, and (4) quality assessment of the resulting structure.[31]

To date, structural information for only three lipoxygenases is available from the Protein Data Bank of Brookhaven (PDB, www.rcsb.org/pdb): two isoforms from soybeans, LOX-1[32] and LOX-3,[33] and one from rabbit reticulocytes, 15-LOX.[34] These share, respectively, 26, 31, and 38% identity with human 5-LOX.

With the highest sequence similarity, rabbit 15-LOX was used as template for the homology model of human 5-LOX. The target-template alignment is recognized as the most critical step in homology modeling. To improve the accuracy of this essential stage, a "consensus" alignment (Figure 4) between the target and the template sequences was used.[35]

Comparison of numerous LOX amino acid sequences as well as different mutagenesis studies and crystal structures analysis led to the identification of highly conserved residues[36] and important residues, involved in iron chelation,[37,38] protein stability, and positional specificity of oxygenation (substrate positioning).[34,39,40] Confrontation of these experimental data with the proposed alignment allowed assessment of the quality of the consensus alignment, as shown in Figure 4.

The final model has four residues (less than 0.7%) outside the allowed regions of the Ramachandran plot. These are part of loops, far from the active site (Figure 5). It illustrates the difficulty of modeling these flexible parts of proteins.

Although the sequence similarity between LOX isoforms is low, the overall folding pattern is conserved across the available 3D structures and is also recognized in the human 5-LOX model (Figure 5). It is composed of two folding units: a small N-terminal, β-barrel domain, suggested to interact with lipids and a larger C-terminal catalytic domain, mainly composed of α-helices, and containing the active site, i.e., the iron-binding site and the substrate binding cleft.[36,41]

Characterization of the 5-LOX Active Site. The 5-LOX active site consists of a deep bent-shaped cleft containing the non-heme iron cofactor. In agreement with mutagenesis studies,[42] the modeled active site of human 5-LOX is more spacious than that of rabbit 15-LOX (Figure 6). In particular, residues at the bottom of the pocket in 5-LOX (Asn425, Ala424, and Ala603) are smaller than the corresponding ones in 15-LOX (Met419, Ile418, and Ile593). This could partly explain the AA positional specificity of the isoforms. Indeed, in 5-LOX, the fatty acid substrate would slide deeper into the binding pocket than in 15-LOX, approaching its C-7 atom (vs. C-13 atom in 15-LOX) to the hydrogen acceptor (the iron atom) and leading to oxygenation closer to the carboxylate moiety.

Further inspection of the active site reveals specificity regions (Figure 7). The main binding cleft extends from Phe177 and Tyr181, in the upper part, to Trp599 and Leu420, at the bottom.

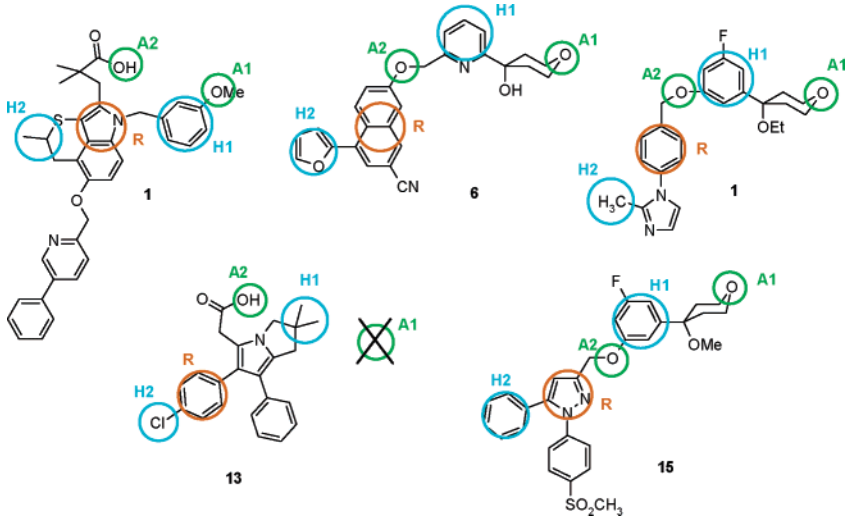

Figure 3. 2D mapping of the pharmacophoric features onto compounds representative of each family. The features are color-coded as follow: hydrophobic group (H) in cyan, ring aromatic (R) in orange, and hydrogen bond acceptor (A) in green.

```
15LOX:   2 GVYRVCVSTGASIYAGSKNKVELWLVGQHGEVELGSCLRP-----TRNKEEE   48
5LOX:    1 PSYTVTVATGSQWFAGTDDYIYLSLVGSAGCSEKHLLDKPFYNDFERGAVDS   52

15LOX:  49 FKVNVSKYLGSLLFVRLRKKHFLKEDAWFCNWISVQALGAAEDKYWFPCYRW  100
5LOX:   53 YDVTVDEELGEIQLVRIEKRKYWLNDDWYLKYITLKTPH--GDYIEFPCYRW  102

15LOX: 101 VVGDGVQSLPVGTGCTTVGDPQGLFQKHREQELEERRKLYQWGSWKEGLILN  152
5LOX:  103 ITGDVEVVLRDGRAKLARDDQIHILKQHRRKELETRQKQYRWMEWNPGFPLS  154

15LOX: 153 VAGSKLTDLPVDERFLEDKKIDFEASLAWGLAELALKNSLNIL-APWKTLDD  203
5LOX:  155 IDAKCHKDLPRDIQFDSEKGVDFVLNYSKAMENLFINRFMHMFQSSWNDFAD  206

15LOX: 204 FNRIFWCGRSKLARRVRDSWQEDSLFGYQFLNGANPMLLRRSVQLPARLVFP  255
5LOX:  207 FEKIFVKISNTISERVMNHWQEDLMFGYQFLNGCNPVLIRRCTELPEKLPVT  258

15LOX: 256 PGMEEL----QAQLEKELKAGTLFEADFALLDNIKANVILY-CQQYLAAPLV  302
5LOX:  259 TEMVECSLERQLSLEQEVQQGNIFIVDFELLDGIDANKTDPCTLQFLAAPIC  310

15LOX: 303 MLKLQPDGKLMPMVIQLHLPKIGSSPPPLFLPTDPPMVWLLAKCWVRSSDFQ  354
5LOX:  311 LLYKNLANKIVPIAIQLN--QIPGDENPIFLPSDAKYDWLLAKIWVRSSDFH  360

                 *   *
15LOX: 355 VHELNSHLLRGHLMAEVFTVATMRCLPSIHPVFKLIVPHLRYTLEINVRARN  406
5LOX:  361 VHQTITHLLRTHLVSEVFGIAMYRQLPAVHPIFKLLVAHVRFTIAINTKARE  412

15LOX: 407 GLVSDFGIFDQIMSTGGGGHVQLLQQAGAFLTYRSFCPPDDLADRGL---LG  455
5LOX:  413 QLICECGLFDKANATGGGGHVQMVQRAMKDLTYASLCFPEAIKARGMESKED  464

15LOX: 456 VESSFYAQDALRLWEIISRYVQGIMGLYYKTDEAVRDDLELQSWCREITEIG  507
5LOX:  465 IPYYFYRDDGLLVWEAIRTFTAEVVDIYYEGDQVVEEDPELQDFVNDVYVYG  516

                                         *   *
15LOX: 508 LQGAQKQGFPTSLQSVAQACHFVTMCIFTCTGQHSSIHLGQLDWFTWVPNAP  559
5LOX:  517 MRGRKSSGFPKSVKSREQLSEYLTVVIFTASAQHAAVNFGQYDWCSWIPNAP  568

15LOX: 560 CTMRLPPPTTK-DATLETVMATLPNLKQSSLQMSIVWQLGRDQPIMVPLGQH  610
5LOX:  569 PTMRAPPPTAKGVVTIEQIVDTLPDRGRSCWHLGAVWALSQFQENELFLGMY  620

                                                          *
15LOX: 611 QEEYFSGPEPRAVLEKFREELAIMDKEIEVRNEKLDIPYEYLRPSIVENSVAI  663
5LOX:  621 PEEHFIEKPVKEAMARFRKNLEAIVSVIAERNKKKQLPYYYLSPDRIPNSVAI  673
```

Figure 4. Consensus alignment of rabbit 15-LOX and human 5-LOX sequences. Parts of the 15-LOX sequence corresponding to breaks in the crystal structure (missing residues) are represented in orange. Highly conserved residues among all LOX isoforms are colored in yellow. Essential sites for iron binding are denoted with an asterisk (∗) whereas residues involved in the positional specificity of oxygenation of AA are colored in magenta.

Both extremities are localized on the surface of the protein. At the entrance, the positively charged residue, Lys409, is thought to interact by salt bridge with the carboxylate moiety of the fatty acid substrate, locking its conformation inside the active site. Most of the residues lining the cavity are hydrophobic. However, a series of probes (GRID program)[43] were used to identify functional groups (HB donor/acceptor, ionic interactions and hydrophobic pockets) potentially involved in inhibitors stabilization. Several polar residues (Gln363, Asn425, Gln557, Ser608, and Arg411) are distributed along the channel and could interact with ligands. A small side pocket also exists, off the main channel. It is composed, among other residues, of Phe421, Gln363, and Leu368 and could accommodate lipophilic groups.

Inhibitors Binding Analysis. The modeled active site was used to investigate the interactions between human 5-LOX and selected inhibitors from the literature, in an attempt to rationalize the available SAR. We explored, through docking studies, the binding modes of five inhibitors, representative of each chemical family, namely compounds **1**, **6**, **11**, **13**, and **15** (Figure 2). SAR data, when available, and the GRID analysis of the active site helped us in the identification of relevant binding modes.

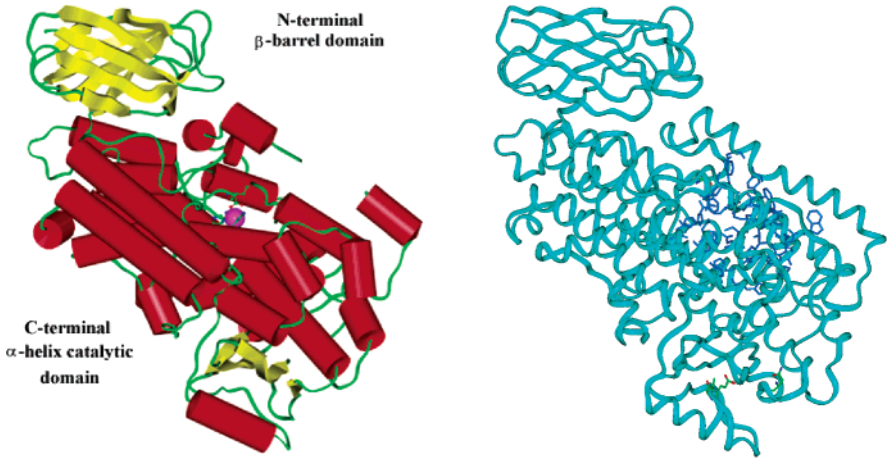

Figure 5. Left: Crystallographic structure of rabbit 15-LOX (PDB entry 1LOX). The iron atom is represented in magenta. Right: Homology modeled structure of human 5-LOX. Active site residues are shown in blue whereas amino acids lying in the disallowed regions of the Ramachandran plot are shown in color by atom type.

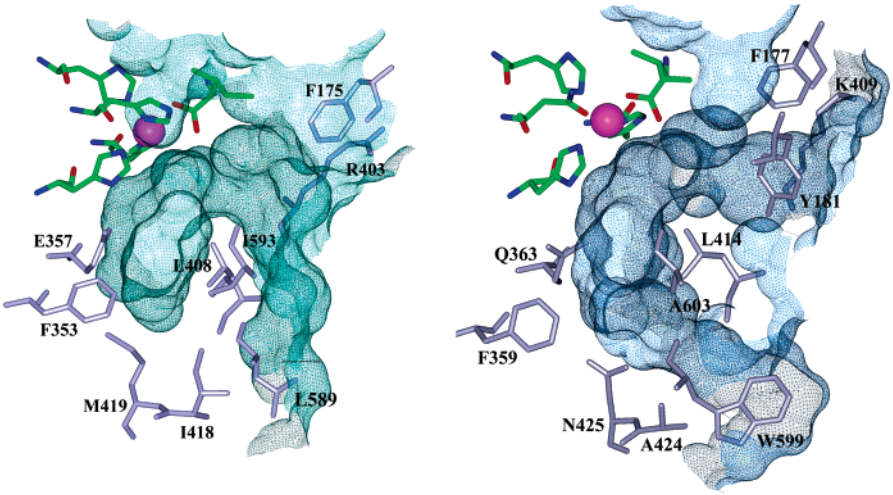

Figure 6. The 15-LOX (left) and modeled 5-LOX (right) active sites and their Connolly surface (probe 1.4 Å), defining the accessible binding pocket. The iron-ligand residues are colored by atom type.

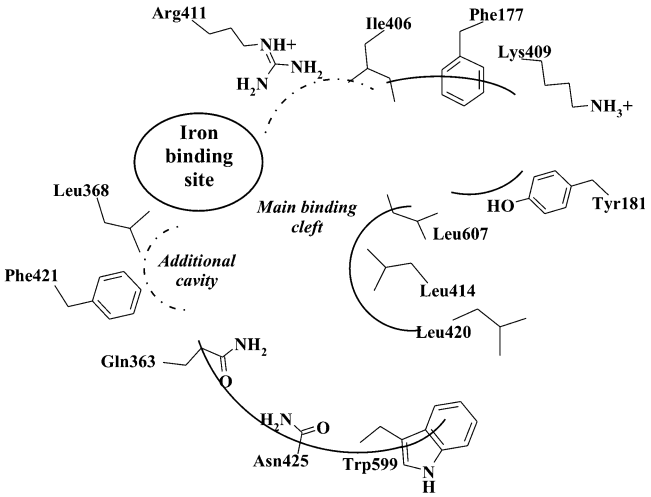

Figure 7. Schematic representation of the human 5-LOX active site.

In general, inside the 5-LOX active site, all the studied compounds adopt a bent-conformation, fitting the shape of the binding cleft. The inhibitors, which are mainly hydrophobic, interact favorably with the lipophilic cavity. However, analysis of the complexes revealed more specific key interactions. Some of these, common to all the compounds, appeared to be important for inhibitory potency.

From our docking approach, one possible binding mode (Figure 8a) was identified for **1** inside the human 5-LOX active site. The inhibitor adopts an extended conformation, fitting perfectly all the binding pockets of the active site. The indole ring lies in a central position, in close proximity to Leu414. The acidic side chain points backward from the main cleft, turning the carboxylate group in the direction of Arg411 (distance O···N = 8.7 Å). Longer side chains would bring these two partners closer and strengthen the salt bridge, resulting in increased binding affinity, as observed among this series.[21] The phenyl-pyridine moiety fits the bottom of the cleft and interacts through H-bonding and CH···π contacts with Asn425 and Trp599, respectively. Positional isomers (ortho and para phenyl substituent), corresponding to less active compounds, would experience steric hindrance with Leu420 and Ala424 residues. The methoxyphenyl moiety fills the hydrophobic pocket at the entrance of the active site. It stabilizes the complex through van der Waals forces that involve, among other residues, Leu607 and Ile406. Replacement of that methoxyphenyl with bigger groups (such as 3-phenylpropyl or 5-phenylpyridin-2-yl) increases the binding affinity, due to better hydrophobic interactions within that pocket. On the contrary, replacement with a methyl group leads to a loss of affinity. Finally, the methyl substituent of the thiopyran ring inserts in the additional cavity and forms CH···π interactions with the lateral chain of Phe421.

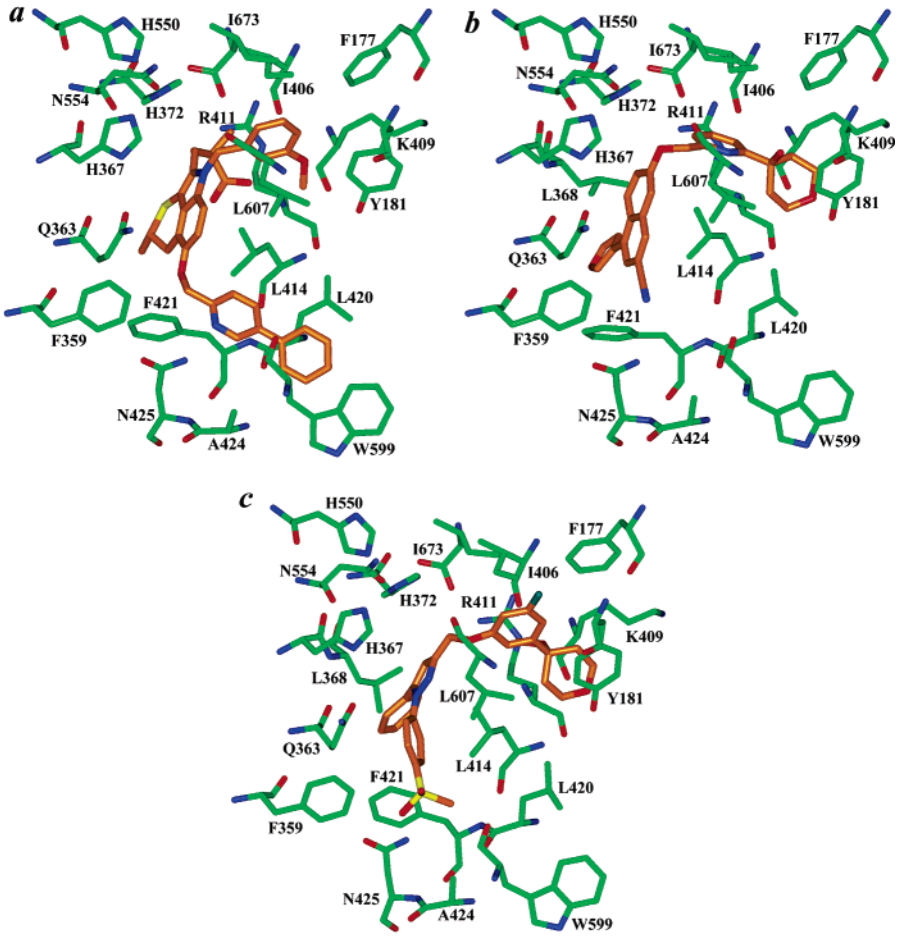

Figure 8. Docking of compounds **1** (a), **6** (b) and **15** (c) inside the human 5-LOX active site.

Figure 8b reports the binding mode of **6** inside the 5-LOX active site. The naphthalene ring is positioned in the middle of the cavity, interacting strongly with Leu414. The nitrile moiety points toward the bottom of the cleft and realizes H-bonding interaction with Asn425 while the furan fills the small hydrophobic pocket delimited, among others, by Phe421 and Leu368. The pyridinic ring lies in the lipophilic region adjacent to the iron-binding center and interacts favorably with Leu607 (CH···O interaction) and Ile406. Finally, the tetrahydropyran ring is positioned such that it participates in a hydrogen bond with Tyr181.

The analysis of the complex formed between **15** and the 5-LOX active site highlights major interaction points, similar to those observed for **6** (Figure 8c). Indeed, the inhibitor fills the active site in an analogous manner. The unsubstituted phenyl ring interacts favorably with the hydrophobic residues delimiting the small additional pocket whereas the fluorophenyl-tetrahydropyran moiety fits the entrance of the active site. Key interactions involve a strong hydrogen bond between the tetrahydropyran oxygen atom and Tyr181 and a second one, weaker, between the sulfone and Asn425. This corroborates experimental results, revealing the essential and secondary roles played by the tetrahydropyran and the sulfone, respectively.[26] CH···π contacts are also observed between the pyrazole ring and Leu414.

Imidazolic derivatives (**11** and **12**) are characterized by an imidazolylphenyl scaffold with the tetrahydropyran fragment characteristic of ZD-2138 attached in para. Fewer SAR data are available in the literature for this series. However, the binding mode identified for compound **11** (Figure 9) is in agreement with the interaction pattern revealed for the other inhibitors. Indeed, similar key interactions stabilize the inhibitor within the binding cleft. Two strong hydrogen bonds are realized between the tetrahydropyran oxygen and Tyr181, and, the imidazolic nitrogen and Asn425, respectively. Furthermore, Leu414 interacts through CH···π contact with the phenyl ring.

Licofelone **13** is smaller than the other studied compounds and few SAR data are described that could help in identifying significant anchoring points. Therefore, it has been harder to identify a single binding pose for that compound. Whereas it has been suggested to mimic arachidonic acid bound to 5-LOX, i.e., in the "horseshoe" conformation,[44] **13** seems to be too constrained to fill the active site as arachidonate would do. However, the carboxylate end is directed toward Arg411 at the back wall of the active site (distance O···N = 8.3 Å). The chlorophenyl ring is stabilized favorably within the additional lipophilic pocket while the dihydropyrrolizine group interacts through CH···π contacts with Leu414.

Confrontation of the Docking Results with the Pharmacophore Model: toward an Interaction Model within the 5-LOX Active Site. In an attempt to assess the pharmacophore model with regard to the docking results, the inhibitors in their "bioactive" conformation (i.e. bound to 5-LOX) were superimposed to their 3D mapping onto the pharmacophore hypothesis. For all the studied compounds except **1**, both conformations are generally quite well overlaid. This observation confirms that the proposed pharmacophore model can fit the binding cavity and matches well with the topology of the active site. Four of the five pharmacophore points correspond to highly conserved interaction sites identified during the molecular docking analysis. Indeed, the aromatic ring (R), mapped by groups such as indole, naphthalene, imidazole, or phenyl, lies in the middle of the cleft

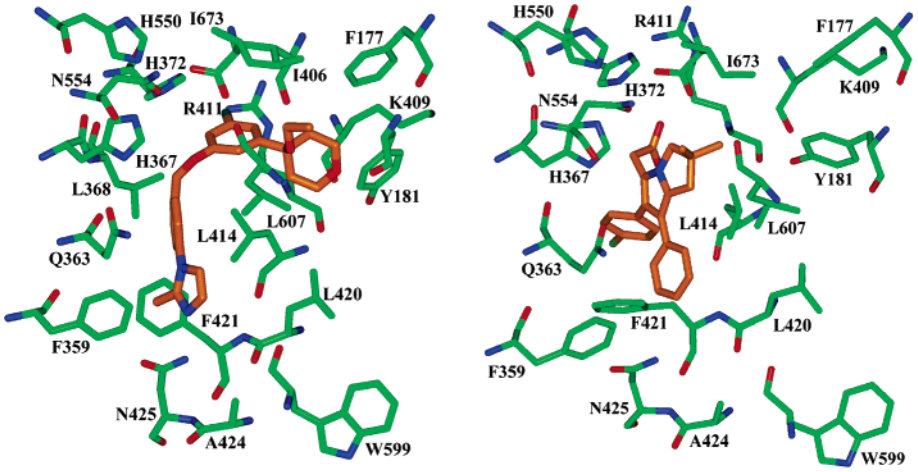

Figure 9. Docking of compounds **11** (left) and **13** (right) inside the human 5-LOX active site.

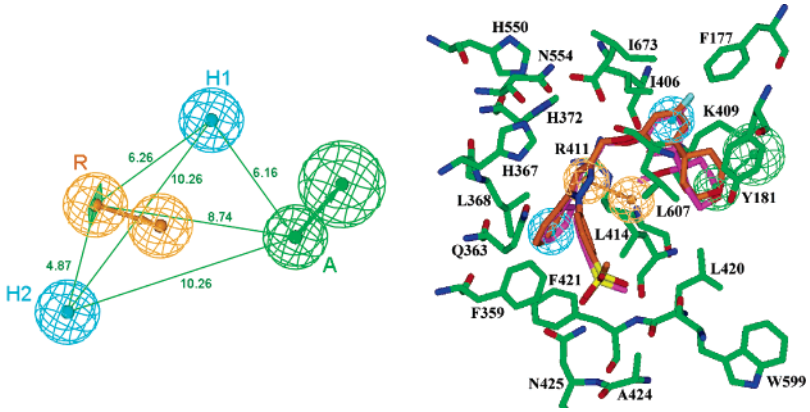

Figure 10. Left: Refined pharmacophore hypothesis. The pharmacophore features are color coded as follow: hydrogen bond acceptor (A) in green, hydrophobic features (H) in cyan and aromatic ring (R) in orange. Distances between the features are expressed in Å, with a tolerance of ± 0.8 Å. Right: Refined pharmacophore hypothesis mapped with **15** (in magenta) superimposed onto the docked conformation (in orange) of **15** inside the 5-LOX active site.

and interacts strongly with Leu414 through CH···π contacts. One of the hydrophobic groups (H2) accommodates the small lipophilic side pocket surrounded by Phe421 and Leu368, while the other (H1) is located at the upper part of the binding site, in close proximity to Ile406 and Leu607. The first hydrogen bond acceptor (A1) fits the entrance of the active site and realizes an H-bonding interaction with Tyr181. In contrast, the second hydrogen bond acceptor (A2), principally mapped by ether oxygen atoms, does not find its counterpart in the active site of 5-LOX; no hydrogen bond donor residue can be seen in its surrounding. Therefore, it is suggested that this point is not an essential feature for optimal interaction with the enzyme but rather serves as a spacer moiety that is common to a majority of the studied compounds.

To refine the pharmacophore, structural information derived from the 5-LOX homology model and the docking results was incorporated in the pharmacophore generation. In fact, the docked conformation of **1**, **6**, **11**, **13**, and **15** were added to the conformational models imported into Catalyst and 10 new pharmacophore hypotheses were produced. They all consisted of four features and had scores ranging from 230 to 240. Based on hierarchical clustering, two main groups can be distinguished among these: RHHA and RRHA. At first sight, it can be noticed that all the hypotheses contain one hydrogen bond acceptor only. Deeper analysis revealed that the ninth hypothesis (RHHA) gives the best correlation between the inhibitors mapping and the docking results (Figure 10).

Moreover, based on the analysis of the docked complexes, two other anchoring points can be mentioned: an acidic moiety (negatively ionizable group), characteristic of the thiopyranindolic derivatives, able to interact with Arg411 as well as a hydrogen bond acceptor close to Asn425. These features were not underlined during the pharmacophore generation because they are not shared by all the inhibitors. However, one could take advantage of these additional secondary interaction points in the design of new inhibitors. Thus, the proposed target-based pharmacophore model involves four principal and two secondary chemical features (Figure 11).

Conclusion

In an attempt to understand the molecular interaction between non redox inhibitors and human 5-LOX, we developed a pharmacophore model consisting of five chemical features: an aromatic ring, two hydrophobic groups and two hydrogen bond acceptors (RHHAA). It corroborates well the available SAR. However, to consider structural information about the target as well, a theoretical 3D model of human 5-LOX was elaborated by homology with rabbit 15-LOX, based on a consensus alignment of the sequences. The 5-LOX active site was then characterized from a structural point of view and used to study the docking of selected representative inhibitors. This shed new light on the binding features of the enzyme. Combination of the pharmacophore model and the results from the docking studies allowed us to weight the different pharmacophoric

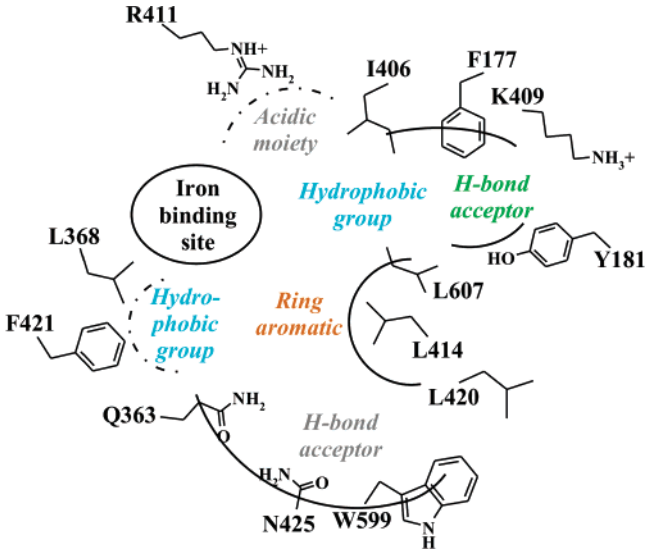

Figure 11. Target-based pharmacophore of 5-LOX non redox inhibitors consisting of four major anchoring points (identified by pharmacophore modeling, colored accordingly) and two secondary ones (identified through docking, colored in gray).

features and to identify and reject one of the hydrogen bond acceptors, rather playing a role of spacer than of essential anchoring point. This was further confirmed by the refined pharmacophore (RHHA), resulting from the addition of the docking conformations to the conformational models. Moreover, two additional interaction points, consisting in an acidic moiety, able to interact with Arg411, and a hydrogen bond acceptor located close to Asn425, were added to the model. It led to the proposal of an interaction model inside the 5-LOX active site, involving four major pharmacophoric features: two hydrophobic groups, a hydrogen bond acceptor, and an aromatic ring, and two secondary ones, an acidic moiety and a hydrogen bond acceptor. Key anchoring points inside the binding cavity include, among others, Tyr181, Leu414, Asn425, Arg411, and Phe421. The present study is a first step toward the characterization of human 5-LOX and its interaction with ligands. We would like to encourage prospective experimental groups to carry out mutagenesis studies on the residues pointed out as key interaction sites for non redox inhibitors. Fundamental understanding of the molecular details of inhibitors/5-LOX interactions remains very rudimentary, in contrast with the extensive studies carried out on the localization and activation of the enzyme.

Furthermore, this target-based pharmacophore could be used soon as a database query to identify potential new non redox 5-LOX inhibitors. Preliminary virtual screening, based on this pharmacophore, has already been performed leading to the identification of some candidates, characterized for example by a phenylthiourea moiety or a pyrimidine-5-carboxylate group. These compounds and analogues will now be evaluated for their potency against 5-LOX.

Computational Methods

All computational experiments were conducted on a Silicon Graphics Octane2 workstation, running under the IRIX 6.5 operating system.

Pharmacophore Modeling. The inhibitors of the training set were modeled by means of the Builder module in InsightII[45] and their geometry optimized by molecular mechanics using CFF91 force field (ESFF force field was used for compounds **4** and **5** as they contain a deprotonated sulfonamide and tetrazole moiety, respectively, that cannot be modeled with CFF91). Conformational models of the molecules were generated through molecular dynamics with the Discover3 module[46] in InsightII. The simulation was performed at 1000K during a period of 10000 fs, with a 1 fs time step. Then, simulated annealing (down to 300K) and subsequent energy minimization followed. This latter consists of three sequential steps using two first-order algorithms, the Steepest Descent (convergence criteria: 10 kcal·mol^{-1}·Å^{-1}) and Conjugate Gradient (0.01 kcal·mol^{-1}·Å^{-1}) and a second-order one, the Newton−Raphson (0.001 kcal·mol^{-1}·Å^{-1}). A distance dependent dielectric constant (1**r*) was chosen. A maximum of 250 conformations for each molecule was generated to ensure maximum coverage of the conformational space. They were then clustered in families based on a root-mean-square deviation (RMSD) value of 0.5 Å, and only conformations within 10 kcal·mol^{-1} from the minimum energy conformation were kept for further work.

Molecules with their conformational models were then imported into the Catalyst software package[47] (version 4.9) and submitted to the HipHop algorithm for pharmacophore hypothesis generation. HipHop provides 3D feature-based alignments for a set of preferably diverse and highly active compounds, without considering activity. These hypotheses are produced by comparing the collection of conformational models and a selection of chemical features shared among the training set molecules. Therefore, the produced pharmacophore hypotheses correspond to the distribution in 3D space of chemical features that are common to the set of input molecules. Each chemical feature is surrounded by a certain spatial tolerance sphere. A compound matches the hypothesis if it possesses conformations and structural features that can be superimposed within a certain tolerance from the corresponding ideal locations. Hydrogen bond acceptors, donors, and aromatic rings additionally include a vector and a second sphere, defining the direction and site of the interaction.

In this study, an initial analysis revealed that four chemical feature types, i.e., hydrogen bond acceptor (A), hydrophobic (H), hydrophobic aromatic (Z), and aromatic ring (R), could effectively map all molecules in our training set. A total of 10 pharmacophore hypotheses were produced. The highest weighting was given to compounds **7** and **11**. These are the most rigid molecules, among the training set, that possess all the chemical features. For these two inhibitors, the "Principal" value was set to 2 (vs 1 for the other inhibitors) and the "Maximum Omitted Features" value was set to 0 (vs 1 for the others). In the hypothesis generation methodology, default settings were used, except the tolerance factor, set to a value of 0.8 instead of 1.0, and the Misses option, set to 2 instead of 0. This latter option controls the number of molecules in the training set that do not have to map all features in generated hypotheses. This parameter was put to a value of 2 to allow compounds **13** and **14**, smaller than the other input inhibitors, to miss mapping to all of the features in an output hypothesis. Finally, the "catHypo.forceAbsoluteStereochemistry" parameter was set to 1 to force the automatic hypothesis routines to consider only the supplied configurations and no enantiomers.

Homology Modeling. The human 5-LOX sequence was obtained from Swiss-Prot database (accession number P09917). Sequence analysis was performed using BLAST[48] through the Protein Data Bank (BLOSUM62 matrix). Rabbit 15-LOX (PDB code 1LOX)[34] was selected as the most appropriate template (sequence identity with human 5-LOX higher than 30%). Both amino acid sequences were aligned by means of the EsyPred3D program (available at www.fundp.ac.be/urbm/bioinfo/esypred/).[35] This automated homology modeling program compares results from various multiple alignment algorithms (such as PSI−BLAST, ClustalW, Dialign2, etc) to derive a "consensus" alignment between the target sequence and the template one. Furthermore, a 3D model (built with Modeler) was also provided with EsyPred3D. However, on the basis of the consensus alignment, we preferred to build the model step by step with the Homology package[49] from InsightII. Indeed, the X-ray data set of rabbit 15-LOX is incomplete and its 3D structure exhibits several breaks (see Figure 5). These could not be correctly modeled by EsyPred3D (one helix missing, see Supporting Information).

The resulting model was then energy-minimized using the CVFF forcefied (Discover3/InsightII). During the optimization, the iron-

ligand residues (His367, His372, His550, Asn554, and Ile673) were held fixed in order to preserve the octahedral geometry of the metal binding site. Quality verification of the model was performed with Procheck 3.0 program with a pseudo-resolution of 2.0 Å.[50]

Active Site Exploration. Based on the superimposition of rabbit 15-LOX and human 5-LOX 3D structures, the 5-LOX active site was defined as a sphere of 12.5 Å radius centered on the inhibitor cocrystallized with rabbit 15-LOX.

The Connolly surface of the active site, representative of the accessible binding-pocket, was calculated by means of a 1.4 Å probe in InsightII. Furthermore, the active site of the modeled enzyme was explored by means of several GRID probes (version 2.2),[43] representative of functional groups of the inhibitors. The probes used were methyl (C3), furan oxygen (OC2), chlorine atom (CL), multi-atom carboxy (COO-), hydrophobic (DRY), and sulfone (OS). The contour maps, corresponding to the most favorable positions, were visualized using the contour facility of InsightII. Calculations were performed on a sphere (15.0 Å radius) centered on the active site, with a grid spacing of 1.0 Å. The interaction energy between the probe and every atom within the protein structure was evaluated at each grid point.

Docking Studies. Docking of the inhibitors (**1**, **6**, **11**, **13**, and **15**) into human 5-LOX was carried out using GOLD[51] (version 1.1) and AutoDock[52] (version 3.0) programs. GOLD is based on a genetic algorithm. It performs docking of flexible ligands into proteins with partial flexibility in the neighborhood of the active site. The torsion angles of Ser, Thr, and Tyr hydroxyl groups as well as Lys NH_3^+ moieties are optimized during the run so that hydrogen bond formation is favored. Default settings were used for the genetic algorithm parameters. AutoDock implements a Lamarckian Genetic Algorithm (LGA) (genetic algorithm coupled with a local search). The protocol applied involves a maximum number of 300000 energy evaluations, a mutation rate of 0.02, a crossover rate of 0.8, and an elitism value of 1. Two hundred independent docking runs were carried out for each ligand. Results differing by less than 2.0 Å in positional RMSD were clustered together and represented by the result with the most favorable free energy of binding.

Display and examination of the complexes was carried out using the InsightII environment. The binding hypothesis, common to both docking programs and in agreement with the inhibitors' SAR and GRID molecular interaction fields, was selected. To take into account protein flexibility, the complexes were then refined with Discover3 (CVFF force field, dielectric constant = 1**r*). The energetic minimization process consists of two sequential steps: the Steepest Descent algorithm, reaching a convergence of 10.0 kcal·mol^{-1}·Å^{-1}, followed by the Conjugate Gradient one to reach a final convergence of 0.01 kcal·mol^{-1}·Å^{-1}. First, all the protein's atoms were held fixed, and only the orientation of the inhibitor was optimized. Then, the α-C atoms of the receptor's residues (sphere of 12.5 Å radius, defined in the active site exploration section) were relaxed. A tethering restraint was applied on these atoms, to keep them from moving too far from their original positions. This restraint had a quadratic form with a constant force of 20 kcal·Å^{-2} and was progressively decreased (scale factors of 0.5 and 0.25).

Acknowledgment. C. Charlier is greatly indebted to the Belgian National Foundation for Scientific Research (FNRS) for the award of a research fellowship.

Supporting Information Available: Representation of the human 5-LOX model automatically provided by EsyPred3D and Ramachandran map of the human 5-LOX model (built with the aid of Homology). This material is available free of charge via the Internet at http://pubs.acs.org.

References

(1) Brash, A. R. Lipoxygenases: occurrence, functions, catalysis, and acquisition of substrate. *J. Biol. Chem.* **1999**, *274*, 23679−23682.
(2) Shibata, D.; Axelrod, B. Plant lipoxygenases. *J. Lipid. Mediat. Cell Signal.* **1995**, *12*, 213−228.
(3) Porta, H.; Rocha-Sosa, M. Lipoxygenase in bacteria: a horizontal transfer event? *Microbiology* **2001**, *147*, 3199−3200.
(4) Vance, R. E.; Hong, S.; Gronert, K.; Serhan, C. N.; Mekalanos, J. J. The opportunistic pathogen Pseudomonas aeruginosa carries a secretable arachidonate 15-lipoxygenase. *Proc. Natl. Acad. Sci. U.S.A.* **2004**, *101*, 2135−2139.
(5) Kuhn, H. Structural basis for the positional specificity of lipoxygenases. *Prostaglandins Other Lipid Mediat.* **2000**, *62*, 255−270.
(6) Radmark, O. Arachidonate 5-lipoxygenase. *Prostaglandins Other Lipid Mediat.* **2002**, *68*−*69*, 211−234.
(7) Samuelsson, B. Leukotrienes: mediators of immediate hypersensitivity reactions and inflammation. *Science* **1983**, *220*, 568−575.
(8) Samuelsson, B.; Dahlen, S. E.; Lindgren, J. A.; Rouzer, C. A.; Serhan, C. N. Leukotrienes and lipoxins: structures, biosynthesis, and biological effects. *Science* **1987**, *237*, 1171−1176.
(9) Brain, S. D.; Williams, T. J. Leukotrienes and inflammation. *Pharmacol. Ther.* **1990**, *46*, 57−66.
(10) Wenzel, S. E. The role of leukotrienes in asthma. *Prostaglandins Leukot. Essent. Fatty Acids* **2003**, *69*, 145−155.
(11) Romano, M.; Claria, J. Cyclooxygenase-2 and 5-lipoxygenase converging functions on cell proliferation and tumor angiogenesis: implications for cancer therapy. *FASEB J.* **2003**, *17*, 1986−1995.
(12) Ding, X. Z.; Hennig, R.; Adrian, T. E. Lipoxygenase and cyclooxygenase metabolism: new insights in treatment and chemoprevention of pancreatic cancer. *Mol. Cancer* **2003**, *2*, 10.
(13) Dwyer, J. H.; Allayee, H.; Dwyer, K. M.; Fan, J.; Wu, H.; Mar, R.; Lusis, A. J.; Mehrabian, M. Arachidonate 5-lipoxygenase promoter genotype, dietary arachidonic acid, and atherosclerosis. *N. Engl. J. Med.* **2004**, *350*, 29−37.
(14) Mehrabian, M.; Allayee, H. 5-lipoxygenase and atherosclerosis. *Curr. Opin. Lipidol.* **2003**, *14*, 447−457.
(15) Young, R. N. Inhibitors of 5-lipoxygenase: a therapeutic potential yet to be fully realized? *Eur. J. Med. Chem.* **1999**, *34*, 671−685.
(16) Julemont, F.; Dogne, J. M.; Laeckmann, D.; Pirotte, B.; de Leval, X. Recent developments in 5-lipoxygenase inhibitors. *Expert Opin. Ther. Pat.* **2003**, *13*, 1−13.
(17) Charlier, C.; Michaux, C. Dual inhibition of cyclooxygenase-2 (COX-2) and 5-lipoxygenase (5-LOX) as a new strategy to provide safer non-steroidal anti-inflammatory drugs. *Eur. J. Med. Chem.* **2003**, *38*, 645−659.
(18) Lewis, T. A.; Bayless, L.; DiPesa, A. J.; Eckman, J. B.; Gillard, M.; Libertine, L.; Scannell, R. T.; Wypij, D. M.; Young, M. A. 5-Lipoxygenase inhibition by N-hydroxycarbamates in dual-function compounds. *Bioorg. Med. Chem. Lett.* **2005**, *15*, 1083−1085.
(19) Lewis, T. A.; Bayless, L.; Eckman, J. B.; Ellis, J. L.; Grewal, G.; Libertine, L.; Marie Nicolas, J.; Scannell, R. T.; Wels, B. F.; Wenberg, K.; Wypij, D. M. 5-Lipoxygenase inhibitors with histamine H1 receptor antagonist activity. *Bioorg. Med. Chem. Lett.* **2004**, *14*, 2265−2268.
(20) McMillan, R. M.; Walker, E. R. Designing therapeutically effective 5-lipoxygenase inhibitors. *Trends Pharmacol. Sci.* **1992**, *13*, 323−330.
(21) Hutchinson, J. H.; Riendeau, D.; Brideau, C.; Chan, C.; Delorme, D.; Denis, D.; Falgueyret, J. P.; Fortin, R.; Guay, J.; Hamel, P.; Jones, T. R.; Macdonald, D.; McFarlane, C. S.; Piechuta, H.; Scheigetz, J.; Tagari, P.; Thérien, M.; Girard, Y. Substituted thiopyrano[2,3,4-c,d]-indoles as potent, selective, and orally active inhibitors of 5-lipoxygenase. Synthesis and biological evaluation of L-691,816. *J. Med. Chem.* **1993**, *36*, 2771−2787.
(22) Hamel, P.; Riendeau, D.; Brideau, C.; Chan, C. C.; Desmarais, S.; Delorme, D.; Dube, D.; Ducharme, Y.; Ethier, D.; Grimm, E.; Falgueyret, J. P.; Guay, J.; Jones, T. R.; Kwong, E.; McAuliffe, M.; McFarlane, C. S.; Piechuta, H.; Roumi, M.; Tagari, P.; Young, R. N.; Girard, Y. Substituted (pyridylmethoxy)naphthalenes as potent and orally active 5- lipoxygenase inhibitors; synthesis, biological profile, and pharmacokinetics of L-739,010. *J. Med. Chem.* **1997**, *40*, 2866−2875.
(23) Mano, T.; Okumura, Y.; Sakakibara, M.; Okumura, T.; Tamura, T.; Miyamoto, K.; Stevens, R. W. 4-[5-Fluoro-3-[4-(2-methyl-1*H*-imidazol-1-yl)benzyloxy]phenyl]-3,4,5,6-tetrahydro-2*H*-pyran-4-carboxamide, an Orally Active Inhibitor of 5-Lipoxygenase with Improved Pharmacokinetic and Toxicology Characteristics. *J. Med. Chem.* **2004**, *47*, 720−725.
(24) Laufer, S. A.; Augustin, J.; Dannhardt, G.; Kiefer, W. (6,7-Diaryldihydropyrrolizin-5-yl)acetic acids, a novel class of potent dual inhibitors of both cyclooxygenase and 5-lipoxygenase. *J. Med. Chem.* **1994**, *37*, 1894−1897.
(25) Ding, C.; Cicuttini, F. Licofelone (Merckle). *IDrugs* **2003**, *6*, 802−808.

(26) Pommery, N.; Taverne, T.; Telliez, A.; Goossens, L.; Charlier, C.; Pommery, J.; Goossens, J. F.; Houssin, R.; Durant, F.; Henichart, J. P. New COX-2/5-LOX inhibitors: apoptosis-inducing agents potentially useful in prostate cancer chemotherapy. *J. Med. Chem.* **2004**, *47*, 6195−6206.
(27) Barbey, S.; Goossens, L.; Taverne, T.; Cornet, J.; Choesmel, V.; Rouaud, C.; Gimeno, G.; Yannic-Arnoult, S.; Michaux, C.; Charlier, C.; Houssin, R.; Henichart, J. P. Synthesis and activity of a new methoxytetrahydropyran derivative as dual cyclooxygenase-2/5-lipoxygenase inhibitor. *Bioorg. Med. Chem. Lett.* **2002**, *12*, 779−782.
(28) Hutchinson, J. H.; Charleson, S.; Evans, J. F.; Falgueyret, J. P.; Hoogsteen, K.; Jones, T. R.; Kargman, S.; Macdonald, D.; McFarlane, C. S.; Nicholson, D. W.; Piechuta, H.; Riendeau, D.; Scheigetz, J.; Thérien, M.; Girard, Y. Thiopyranol[2,3,4-*c*,*d*]indoles as inhibitors of 5-lipoxygenase, 5-lipoxygenase-activating protein, and leukotriene C4 synthase. *J. Med. Chem.* **1995**, *38*, 4538−4547.
(29) Ducharme, Y.; Brideau, C.; Dube, D.; Chan, C. C.; Falgueyret, J. P.; Gillard, J. W.; Guay, J.; Hutchinson, J. H.; McFarlane, C. S.; Riendeau, D.; Scheigetz, J.; Girard, Y. Naphthalenic lignan lactones as selective, nonredox 5-lipoxygenase inhibitors. Synthesis and biological activity of (methoxyalkyl)thiazole and methoxytetrahydropyran hybrids. *J. Med. Chem.* **1994**, *37*, 512−518.
(30) Dube, D.; Blouin, M.; Brideau, C.; Chan, C. C.; Desmarais, S.; Ethier, D.; Falgueyret, J. P.; Friesen, R. W.; Girard, M.; Girard, Y.; Guay, J.; Riendeau, D.; Tagari, P.; Young, R. N. Quinolines as potent 5-lipoxygenase inhibitors: synthesis and biological profile of L-746,530. *Bioorg. Med. Chem. Lett.* **1998**, *8*, 1255−1260.
(31) Sanchez, R.; Sali, A. Advances in comparative protein-structure modelling. *Curr. Opin. Struct. Biol.* **1997**, *7*, 206−214.
(32) Minor, W.; Steczko, J.; Stec, B.; Otwinowski, Z.; Bolin, J. T.; Walter, R.; Axelrod, B. Crystal structure of soybean lipoxygenase L-1 at 1.4 Å resolution. *Biochemistry* **1996**, *35*, 10687−10701.
(33) Skrzypczak-Jankun, E.; Amzel, L. M.; Kroa, B. A.; Funk, M. O., Jr. Structure of soybean lipoxygenase L3 and a comparison with its L1 isoenzyme. *Proteins* **1997**, *29*, 15−31.
(34) Gillmor, S. A.; Villasenor, A.; Fletterick, R.; Sigal, E.; Browner, M. F. The structure of mammalian 15-lipoxygenase reveals similarity to the lipases and the determinants of substrate specificity. *Nat. Struct. Biol.* **1997**, *4*, 1003−1009.
(35) Lambert, C.; Leonard, N.; De Bolle, X.; Depiereux, E. ESyPred3D: Prediction of proteins 3D structures. *Bioinformatics* **2002**, *18*, 1250−1256.
(36) Prigge, S. T.; Boyington, J. C.; Faig, M.; Doctor, K. S.; Gaffney, B. J.; Amzel, L. M. Structure and mechanism of lipoxygenases. *Biochimie* **1997**, *79*, 629−636.
(37) Zhang, Y. Y.; Lind, B.; Radmark, O.; Samuelsson, B. Iron content of human 5-lipoxygenase, effects of mutations regarding conserved histidine residues. *J. Biol. Chem.* **1993**, *268*, 2535−2541.
(38) Hammarberg, T.; Zhang, Y. Y.; Lind, B.; Radmark, O.; Samuelsson, B. Mutations at the C-terminal isoleucine and other potential iron ligands of 5-lipoxygenase. *Eur. J. Biochem.* **1995**, *230*, 401−407.
(39) Borngraber, S.; Browner, M.; Gillmor, S.; Gerth, C.; Anton, M.; Fletterick, R.; Kuhn, H. Shape and specificity in mammalian 15-lipoxygenase active site. The functional interplay of sequence determinants for the reaction specificity. *J. Biol. Chem.* **1999**, *274*, 37345−37350.
(40) Gan, Q. F.; Browner, M. F.; Sloane, D. L.; Sigal, E. Defining the arachidonic acid binding site of human 15-lipoxygenase. Molecular modeling and mutagenesis. *J. Biol. Chem.* **1996**, *271*, 25412−25418.
(41) Allard, J. B.; Brock, T. G. Structural organization of the regulatory domain of human 5-lipoxygenase. *Curr. Protein Pept. Sci.* **2005**, *6*, 125−131.
(42) Schwarz, K.; Walther, M.; Anton, M.; Gerth, C.; Feussner, I.; Kuhn, H. Structural basis for lipoxygenase specificity. Conversion of the human leukocyte 5-lipoxygenase to a 15-lipoxygenating enzyme species by site- directed mutagenesis. *J. Biol. Chem.* **2001**, *276*, 773−779.
(43) Goodford, P. J. A computational procedure for determining energetically favorable binding sites on biologically important macromolecules. *J. Med. Chem.* **1985**, *28*, 849−857.
(44) Laufer, S. Discovery and development of ML3000. *Inflammopharmacology* **2001**, *9*, 101−112.
(45) Accelrys Inc. *InsightII*; version 2000 ed.: San Diego, CA.
(46) Accelrys Inc. *Discover3*; 2.98 ed.: San Diego, CA.
(47) Accelrys Inc. *Catalyst*; version 4.9 ed.: San Diego, CA.
(48) Altschul, S. F.; Madden, T. L.; Schaffer, A. A.; Zhang, J.; Zhang, Z.; Miller, W.; Lipman, D. J. Gapped BLAST and PSI−BLAST: a new generation of protein database search programs. *Nucleic Acids Res.* **1997**, *25*, 3389−3402.
(49) Biosym/MSI. *Homology, User guide*; San Diego, CA, 1993.
(50) Laskowski, R. A. Procheck: a program to check the stereochemical quality of protein structures. *J. Appl. Crystallogr.* **1993**, *26*, 283−291.
(51) Jones, G.; Willett, P.; Glen, R. C.; Leach, A. R.; Taylor, R. Development and validation of a genetic algorithm for flexible docking. *J. Mol. Biol.* **1997**, *267*, 727−748.
(52) Morris, G. M.; Goodsell, D. S.; Halliday, R. S.; Huey, R.; Hart, W. E.; Belew, R. K.; Olson, A. J. Automated docking using a Lamarckian genetic algorithm and an empirical binding free energy function. *J. Comput. Chem.* **1998**, *19*, 1639−1662.

JM050870X